IRIS AperTO

UNIVERSITÀ DEGLI STUDI DI TORINO

AperTO - Archivio Istituzionale Open Access dell'Università di Torino

**Sonoluminescence and acoustic emission spectra at different stages of cavitation zone development**

**This is the author's manuscript**

*Original Citation:*

*Availability:*

This version is available http://hdl.handle.net/2318/1636415 since 2018-03-27T12:00:55Z

*Published version:*

DOI:10.1016/j.ultsonch.2017.04.004

*Terms of use:*

Open Access

Anyone can freely access the full text of works made available as "Open Access". Works made available under a Creative Commons license can be used according to the terms and conditions of said license. Use of all other works requires consent of the right holder (author or publisher) if not exempted from copyright protection by the applicable law.

(Article begins on next page)

14 August 2024

IRIS AperTO

UNIVERSITÀ DEGLI STUDI DI TORINO

This Accepted Author Manuscript (AAM) is copyrighted and published by Elsevier. It is posted here by agreement between Elsevier and the University of Turin. Changes resulting from the publishing process - such as editing, corrections, structural formatting, and other quality control mechanisms - may not be reflected in this version of the text. The definitive version of the text was subsequently published in ULTRASONICS SONOCHEMISTRY, None, 2017, 10.1016/j.ultsonch.2017.04.004.

You may download, copy and otherwise use the AAM for non-commercial purposes provided that your license is limited by the following restrictions:

(1) You may use this AAM for non-commercial purposes only under the terms of the CC-BY-NC-ND license.

(2) The integrity of the work and identification of the author, copyright owner, and publisher must be preserved in any copy.

(3) You must attribute this AAM in the following format: Creative Commons BY-NC-ND license (http://creativecommons.org/licenses/by-nc-nd/4.0/deed.en), 10.1016/j.ultsonch.2017.04.004

The publisher's version is available at:
http://linkinghub.elsevier.com/retrieve/pii/S135041771730161X

When citing, please refer to the published version.

Link to this full text:
http://hdl.handle.net/2318/1636415

This full text was downloaded from iris - AperTO: https://iris.unito.it/

iris - AperTO

University of Turin's Institutional Research Information System and Open Access Institutional Repository

# Sonoluminescence and acoustic emission spectra at different stages of cavitation zone development

N.V. Dezhkunov[a,*], A. Francescutto[b], L. Serpe[c], R. Canaparo[c], G. Cravottoc

[a] BSUIR, P. Brovka St. 6, 220013 Minsk, Belarus

[b] Dept of Engineering & Architecture, University of Trieste, 34127 Trieste, Italy

[c] Dept of Drug Science and Technology, University of Turin, 10125 Turin, Italy

Keywords:

Focused ultrasound, Cavitation, Sonoluminescence, Stages of cavitation, Spectra of acoustic emissions

Corresponding author at:

Belarusian State University of Informatics and Radioelectronics (BSUIR), P. Brovka St. 6, 220027 Minsk, Belarus, e-mail address: dnv@bsuir.edu.by (N.V. Dezhkunov).

**Abstract**

The way in which a cavitation zone develops in a focused pulsed ultrasound field is studied in this work. Sonoluminescence (SL), total hydrophone output and cavitation noise spectra have been recorded across a gradual, smooth increase in applied voltage. It is shown that the cavitation zone passes through a number of stages of evolution, according to increasing ultrasound intensity, decreasing pulse period and increasing ultrasound pulse duration. Sonoluminescence is absent in the first phase and the hydrophone output spectra consists of a main line with two or three harmonics whose intensity is much lower than that of the main (fundamental) line. The second stage sees the onset of SL whose intensity increases smoothly and is accompanied by the appearance of higher harmonics and subharmonics in the cavitation noise spectra. In some cases, the wide-band (WBN) component can be seen in noise spectra during the final part of the second stage. In the third stage, SL intensity increases significantly and often quite sharply, while WBN intensity increases in the same manner. This is accompanied by a synchronous increase in the absorption of ultrasound by the cavitation zone, which is manifested in a sharp decrease in the hydrophone output. In the fourth stage, both SL and WBN intensities tend to decrease despite the increased voltage applied to the transducer. Furthermore, the fundamental line tends to decrease in strength as well, despite the increasing ultrasound intensity. The obtained results clearly identify the different stages of cavitation zone development using cavitation noise spectra analyses. We then hypothesize that three of the above stages may be responsible for three known types of ultrasound action on biological cells: damping viability, reversible cell damage (sonoporation) and irreversible damage/cytotoxicity.

## 1. Introduction

High power ultrasound has been used in a number of industrial and chemical fields for quite some time. It is now widely accepted that ultrasound can accelerate physical and chemical processes [1–3], as well as generate specific ultrasonic phenomena, such as the inverse ultrasonic capillary effect [4], and the direct electromotive force [5].

The large number of applications that ultrasound has in experimental and clinical therapies have all received increasing amounts of attention in recent years. This interest is motivated by the promising results obtained during the study of ultrasonically induced biological effects including, I) enhanced cell membrane permeability which improves the delivery of small compounds, macro-molecules and other therapeutics into cells and tissues, i.e. sonoporation [6–9]; II) DNA- mediated transfection [10,11]; III) tumour growth reduction [12,13], and IV) the activation of specific compounds triggering antitumor or antimicrobial activity [14–17]. It is believed that cavitation plays an important role in these bio-effects. Three types of ultrasound action on biological cells have been identified [6–18]; damping viability, reversible cell damage (sonoporation) and irreversible damage/cytotoxicity. It is possible that these types of action derive from the different properties that cavitation displays under different conditions, meaning that the monitoring and control of cavitation is therefore an important factor in the successful use of ultrasound in medicine and biology.

It should be noted that the above effects are non-thermal. One of the possible ways of avoiding overheating when studying the non-thermal effects of ultrasound on biological cells is to use pulsed ultrasound. In fact, the influence of pulse parameters on cavitation activity has been studied in previous works [19–23]. It has been shown, that pulse duration, pulse period and pulse amplitude affect the size distribution of cavitating bubbles and that the cavitation activity that is estimated, for example by sonoluminescence intensity, can be enhanced in pulsed fields when proper pulse parameters are chosen.

Pulsed ultrasound has been used to study the stages of cavitation zone development in this work. We have shown that the cavitation zone passes through a number of stages of evolution (states) according to increasing ultrasound intensity, decreasing pulse period and increasing ultrasound pulse duration. This means that, under stable conditions (when ultrasound intensity and other process parameters are constant), cavitation can be found to be in one of the above states.

## 2. Experimental

The experimental set-up is described in detail elsewhere [23] (Fig. 1).

The experimental chamber was a stainless steel cylinder of 100 mm diameter and 160 mm height. The dissolved gas was air. A focusing 40 mm diameter piezoceramic transducer with a resonance frequency of fo = 720 kHz was mounted on the cell bottom. The hydrophone was placed in the chamber in such a way as to ensure that its spherical sensitive piezoceramic unit (2 mm in diameter and 0.2 mm in wall thickness) was at a distance of 30 mm from the centre of the transducer focal spot. Its output was labelled “H”. The central region of the chamber was viewed using a Ø 25 mm light-guide on a photomultiplier Philips XP 1110, whose output was labelled “L”. The hydrophone and photomultiplier were connected to a Hewlett Packard 54601 multi- channel memory oscilloscope. The hydrophone output was connected to a spectrum analyser, Hewlett Packard E4411B, after preamplification.

In pre-cavitation conditions, the maximum sound pressure measured by the calibrated hydrophone is linearly related to the voltage applied to the transducer; Pmax(bar) = 0.096(bar/V) U(V).

The radiator’s power was supplied by a computer-controlled generator (UZG 08-01, BSUIR, Minsk) equipped with a system of automated resonance frequency tuning. The maximum generator output power of 70 W was achieved at an applied voltage amplitude of 275 Vp-p. The temperature θ of the liquid was continuously monitored by a thermocouple.

The experimental procedure started with the test chamber being filled with distilled water. After being kept in the chamber for 24 h, the liquid was subjected to degassing by ultrasound for 20 min at 170 Vpp transducer voltage (≈10 W/cm$^2$). As a result, the air content decreased by 20–25% of the equilibrium value [23]. The preliminary, partial degassing of the liquid considerably increases the reproducibility of the results since, after treatment, the gas content remains practically unchanged under the influence of ultrasound and during the measurements.

**3. Results and discussion**

Fig. 2 shows the results of the simultaneous measurement of photomultiplier output L (upper panel) and hydrophone output H (lower panel) data, while transducer voltage Up-p was increased linearly by a computer controlled generator, at a rate of 7 V/s.

Hydrophone output H increased linearly with time, over the 5–12.5 s time period, at the beginning of the experiment. This means that any loss of ultrasound energy from absorption by bubbles is negligible, i.e. ultrasound intensity is below the cavitation threshold. The dashed line in Fig. 2 shows how H would be dependent on applied voltage as long as cavitation would be absent.

The slope of the H(t) curve then tended to decrease after 12.5 s, evidently as a result of the cavitation bubbles emerging in the focal zone.

SL emissions (Fig. 2, upper panel) appeared at intensities above those of the background flashes, from approximately the 16th second onwards. This instant is marked on the graph by an arrow and is labelled as Th1 (first threshold of transient cavitation). From this point on, hydrophone output began to pulse across a range of intensities. SL intensity was seen to increase slowly after its appearance (16–26 s).

The deviation of the H(t) curve from the straight dashed line and the distribution of pulse intensities registered by the hydrophone were evidently caused by bubble formation in the focal zone. Both large, stable bubbles and bubbles which were still in the growth phase had the effect of lowering acoustic transparency in the focal region, which may be the reason for the lower peak values of H, whereas collapsing bubbles produce shock waves, which might be the reason for the higher, overall H values.

At another critical voltage, which we shall hereinafter name the second threshold, the slope of L(t) changed considerably and SL intensity rose sharply. This instant in time has been labelled Th2 (second threshold of transient cavitation). Sudden increases in L were accompanied by a widening of the distribution of recorded hydrophone output values. Both maximal and average values of H were observed to drop in a step-wise manner under those conditions. It would appear that this can be accounted for by the onset of an avalanche-like multiplication of cavitation bubbles [20]. Quick growth in the number of active bubbles in this stage leads to an increase in sonoluminescence intensity and to a sharp increase in the loss of ultrasound energy, as caused by absorption in the cavitation zone.

The above results allowed us to identify the following, discrete cavitation zone development stages. During the first stage, SL is absent (Fig. 2, upper record), ultrasound energy absorption is

low and the hydrophone output dispersion of impulses is absent. Rectified diffusion possibly leads to bubbles beginning to grow which slightly increases ultrasound energy absorption and causes the downward deviation of H (t) from the hypothetical dashed line (Fig. 2, lower record).

In the second stage (time period from Th1 to Th2), sonoluminescence appears and is accompanied by the distribution of the hydrophone output. Respective threshold voltages are Uth1 and Uth2. Ultrasound absorption is not much higher here than in stage one. The third stage of cavitation zone development (after Th2) manifests itself in the rapid, and often extremely sharp, increases in both SL intensity and ultrasound absorption by the cavitation zone, the latter of which causes the sharp decrease in hydrophone output at Th2. This stage is usually much shorter than the previous one and would appear to be associated with the onset of an avalanche-like multiplication of cavitation bubbles [24]. The third stage is considered to be finished when the rapid increases are complete and SL intensity variation becomes slow. In the fourth stage, cavitation activity tends towards saturation and may then remain constant or decrease slowly, whereas ultrasound absorption tends to increase. The saturation of cavitation activity following by its decrease with ultrasound intensity increase can be seen in results obtained by authors [25–28].

Figs. 3 and 4 show how SL intensity, L, and hydrophone output, H, depend on pulse duration τ and pulse period T, respectively, when constant voltage is applied to the transducer. Pulse duration, τ (Fig. 3), was increased from its starting point of 0.1 ms, while pulse period, T (Fig. 4), was decreased from T = 1000 ms. Experiments were carried out in this manner in order to decrease the impact of the previous experiment on the results of the subsequent one. The period of exposure to ultrasound, before measurements were made, was 20 s at the chosen U, T and τ values. The rest time between measurements was 30 s.

SL intensity (curves 1) increases, achieves its maximum and then decreases with increasing pulse duration (Fig. 3) and decreasing ultrasound pulse period (Fig. 4). The first thresholds, τth1 and Tth1, are the threshold values of pulse period and pulse duration, respectively, at which SL appears at the given transducer voltage U (150 V,curve 1). The second thresholds, τth2 and Tth2, are the thresholds at which SL intensity increases abruptly. Hydrophone output, H, decreases abruptly at τth2 (Fig. 3) and at Tth2 (Fig. 4) due to an increase of ultrasound energy loss (absorption) in the cavitation zone, which is caused by the increase in bubble volume concentration.

Three stages of cavitation zone development can be identified here in Figs. 3 and 4; the appearance and relatively slow increase in SL intensity, which is accompanied by a slight decrease

in H. Then, we see a rapid increase in SL intensity and sharp increase in ultrasound energy loss, manifested in the decrease in H. Finally, we see L reaching its maximal value and a decrease in SL intensity. The three stages in Figs. 3 and 4 correspond to stages 2, 3 and 4 in Fig. 2. Stage 1 of cavitation zone development is not seen under the experimental conditions in Figs. 3 and 4.

Fig. 5 shows the results of recording hydrophone pulses on a time scale that is comparable with ultrasound pulse duration at the various stages of cavitation zone development, which were collected from Fig. 4. It can be seen that SL intensity grows with ultrasound pulse time over the first two stages (Fig. 5a and b). In stage 3 (Fig. 5c), it grows quickly at the very beginning of the ultrasound pulse, achieves its maximum value and then decreases slowly. The SL intensity maximum is achieved at very beginning of the pulse in stage 4 (Fig. 5d), before then decreasing quickly. This behaviour may be interpreted in terms of cavitation zone oversaturation by bubbles. By “oversaturation”, we intend conditions under which an increase in bubble volume concentration, caused by an increase in voltage applied to the transducer (or ultrasound intensity), an increase in pulse duration or a decrease in ultrasound pulse period, leads to a decrease in SL intensity.

The decrease in cavitation activity under saturation and oversaturation conditions has previously been discussed [24,26,29], and is essentially due to the screening action of the cavitation field and inter- bubble impact. An increase in the intensity of bubble interactions and a simultaneous increase in bubble concentration will increase the probability of bubble deformation and non-spherical collapse; non-spherical collapse is less effective in generating shock waves and high temperatures inside bubbles [29].

The first two cases (Fig. 5a and b) correspond to relatively low ultrasound intensities. Rectified diffusion is slow, while bubble number and size grow slowly and do not achieve the saturation condition during pulse period.

At higher ultrasound intensities (Fig. 5c and d), the saturation of the cavitation zone is achieved at the beginning of the ultrasound pulse, after which the cavitation zone becomes oversaturated with bubbles, leading to a decrease in cavitation activity. The oversaturation of the cavitation zone by bubbles explains the decrease in SL intensity that occurs after maximal values are achieved, i.e. the transition to the fourth stage in the above experiments (Figs. 2–4).

Fig. 6 shows cavitation noise spectra taken at different stages.

Only one peak, $f_0$ (not shown here), was found in the spectra at ultrasound intensities below the cavitation threshold. Peaks $2f_0$ and $3f_0$ may appear in the first stage. In the second stage, higher

harmonics, $nf_0$ (n = 1, 2, 3…), subharmonic, 1/2 $f_0$, and frequencies, $cf(n + 1/2)\ f_0$, can be seen in the spectra. Harmonics up to $(5–7)f_0$ can normally be seen at the second stage. In the third stage, wide-band (WBN) signals appear in the cavitation noise spectrum as well. The stronger the SL intensity is during this stage of cavitation zone development, the higher are the harmonics that can be seen in the spectra and the stronger are their intensities.

The main frequency $f_0$ and the broadband component intensities decrease in the fourth stage (Fig. 5d), while subharmonic intensity increases. The characteristics of the cavitation noise spectrum change essentially as a consequence of the transition from one stage to the other, proving that the different insonation modes can be identified via its spectral analysis.

In summary, it is seen that the cavitation zone in a focused ultrasound field passes through four evolution stages (states) according to increasing ultrasound intensity, decreasing pulse period and increasing ultrasound pulse duration. This means that, under stable conditions, i.e. when ultrasound intensity and other process parameters are constant, cavitation can be found to be in one of the above states. It is possible that the different states of cavitation will have different effects on both the physical and chemical processes that occur in liquids and biological objects.

We therefore hypothesize that a link exists between the three known types of ultrasound action on biological cells, I) damping viability, II) reversible damage of cells (sonoporation), III) irreversible damage/ cytotoxicity, and three of the above cavitation zone development stages, which have been identified and differentiated for the first time in this work. The verification of this hypothesis will be the subject of future work.

## 4. Conclusions

The following stages of cavitation zone development have been identified using the above results:

1. The first stage corresponds to the appearance of cavitation bubbles which pulse at low amplitude in a nonlinear mode. Sound absorption at this stage is not much higher than in the liquid when bubbles are not present, meaning that the bubble volume concentration is low at this stage.

2. SL emissions appear in the second stage. Ultrasound energy loss, or absorbance in other words, is slightly higher in the first stage. Under these conditions, SL intensity is low and rises slowly, while ultrasound intensity increases across a wide range. The growth in both the number and the size of bubbles may be considered the reason for the increase in absorbance.

3. In the third stage, both absorbance and SL intensity grow sharply, indicating that both bubble volume concentration and collapse efficiency increase significantly. SL intensity increases as a result of this transition, by more than one order of magnitude in some cases, while ultrasound absorption more than doubles.

4. In the fourth stage, cavitation activity tends towards saturation and can then remain constant or decrease, whereas ultrasound absorption tends to increase in this stage.

5. The characteristics of the cavitation noise spectrum change essentially as a consequence of the transition from one stage to another and may serve as a means of identifying the various sonication modes.

Acknowledgements

This research was partially supported by the Belarusian Foundation for Fundamental Research and by the University of Trieste.

**References**

[1] A. Weissler, Sonochemistry: the production of chemical changes with sound waves, J. Acoust. Soc. Am. 25 (1953) 651–657.

[2] T.J. Mason, J.P. Lorimer, Applied Sonochemistry, Wiley VCH, Weinheim, 2002. [3] G.I. Eskin, D.G. Eskin, Ultrasonic Treatment of Light Alloy Melts, second ed., CRC Press, Boca Raton, 2014.

[4] N.V. Dezhkunov, G. Iernetti, A. Francescutto, P. Ciuti, Inverse ultrasonic capillary effect, Acoust. Lett. 15 (1993) 202–205.

[5] N.V. Dezhkunov, A. Francescutto, A.I. Kulak, The effect of ultrasonic cavitation on model electrochemical processes, Ultrasonics 34 (1996) 551–553.

[6] R. Karshafian, P.D. Bevan, R. Williams, S. Samac, P.N. Burns, Sonoporation by ultrasound: effect of acoustic exposure parameters on cell membrane permeability and cell viability, Ultrasound Med. Biol. 35 (2009) 847–860.

[7] D.L. Miller, J. Song, Tumor growth reduction and DNA transfer cavitation-enhanced high-intensity focused ultrasound in vivo, Ultrasound Med. Biol. 29 (2003) 887–893.

[8] W.G. Pitt, G.A. Husseini, B.J. Staples, Ultrasonic drug delivery-a general review, Expert Opin. Drug Deliv. 1 (2004) 37–56.

[9] V. Frenkel, Ultrasound mediated delivery of drugs and genes to solid tumors, Adv.Drug Deliv. Rev. 60 (2008) 1193–1208.

[10] S. Koch, P. Pohl, U. Cobet, N.G. Rainov, Ultrasound enhancement of liposome- mediated cell transfection is caused by cavitation effects, Ultrasound Med. Biol. 26 (2000) 897–903.

[11] C.M.H. Newman, T. Bettinger, Gene therapy progress and prospects: ultrasound for gene transfer, Gene Ther. 14 (2007) 465–475.

[12] A.H. Barati, M. Mokhtari-Dizaji, H. Mozdarani, S.Z. Bathaie, Z.M. Hassan, Treatment of murine tumors using dual-frequency ultrasound in an experimental in vivo model, Ultrasound Med. Biol. 35 (2009) 756–763.

[13] J.E. Kennedy, High-intensity focused ultrasound in the treatment of solid tumours, Nat. Rev. Cancer 5 (2005) 321–327.

[14] J.C. Rosenthal, I. Sostaric, Reisz, Sonodynamic therapy – a review of the synergistic effects of drugs and ultrasound, Ultrason. Sonochem. 11 (2004) 349–363.

[15] A.L. Nikolaev, A.V. Gopin, V.E. Bozhevolnov, S.E. Mazina, A.V. Severin, V.N. Rudin, Sonodynamic therapy of cancer. A comprehensive experimental study, Russ. Chem. Bull. 63 (2014) 1036–1047.

[16] F. Foglietta, R. Canaparo, A. Francovich, F. Arena, S. Civerf, G. Cravotto, F. Fraira, L. Serpe, Sonodynamic treatment as an innovative bimodal anticancer approach: shock wave-mediated tumor growth inhibition in a syngeneic breast cancer model, Discovery Med. 20 (2015) 197–205.
[17] C. Mcewman, C. Fowley, N. Nomikou, B. Mccaughan, A.P. Mchale, J.E. Callan, Polymeric microbubbles as delivery vehicles for sensitizers in sonodynamic therapy, Langmuir 30 (2014) 14926.
[18] L. Serpe, F. Giuntini, Sonodynamic antimicrobial chemotherapy: first steps towards a sound approach for microbe inactivation, J. Photochem. Photobiol. 150 (2015) 44–49.
[19] A. Henglein, R. Ulrich, J. Lilie, Luminescence and chemical action by pulsed ultrasound, J. Am. Chem. Soc. 111 (1989) 1974–1979.
[20] M. Ashokkumar, J. Lee, S. Kentish, F. Griezer, Bubbles in an acoustic field: an overview, Ultrason. Sonochem. 9 (2002) 103–106.
[21] A. Brotchie, F. Grieser, M. Ashokkumar, Effect of power and frequency on bubble- size distributions in acoustic cavitation, Phys. Rev. Lett. 102 (2009) 084302.
[22] M. Hauptmann, H. Struyf, S. De Gendt, C. Glorieux, S. Brems, Evaluation and interpretation of bubble size distributions in pulsed megasonic fields, J. Appl. Phys. 113 (2013) 18490.
[23] N.V. Dezhkunov, A. Francescutto, P. Ciuti, T.J. Mason, G. Iernetti, A.I. Kulak, Enhancement of sonoluminescence emission from multibubble cavitation zone, Ultrason. Sonochem. 7 (2000) 19–24.
[24] M.G. Sirotyuk, Acoustic Cavitation, Nauka, Moscow, 2008 (in Russian).
[25] Tu Juan, T.J. Matula, A.A. Brayman, L.A. Crum, Inertial cavitation dose produced in ex vivo rabbit ear arteries with optison by 1-MHz pulsed ultrasound, Ultrasound Med. Biol. 34 (2005) 2009–2018.
[26] N.V. Dezhkunov, Multibubble sonoluminescence intensity dependence on liquid temperature at different ultrasound intensities, Ultrason. Sonochem. 9 (2002) 103–106.
[27] P.B. Subhedar, P.R. Gogate, Enhancing the activity of cellulase enzyme using ultrasonic irradiations, J. Mol. Catal. B Enzym. 101 (2014) 108–114.
[28] I. Tzanakis, G.S.B. Lebon, D.G. Eskin, K. Pericleous, Investigation of the factors influencing cavitation intensity during the ultrasonic treatment of molten alumi- nium, Mater. Des. 90 (2016) 979–983.
[29] T.G. Leighton, The Acoustic Bubble, Academic Press Limited, Cambridge, 1994.

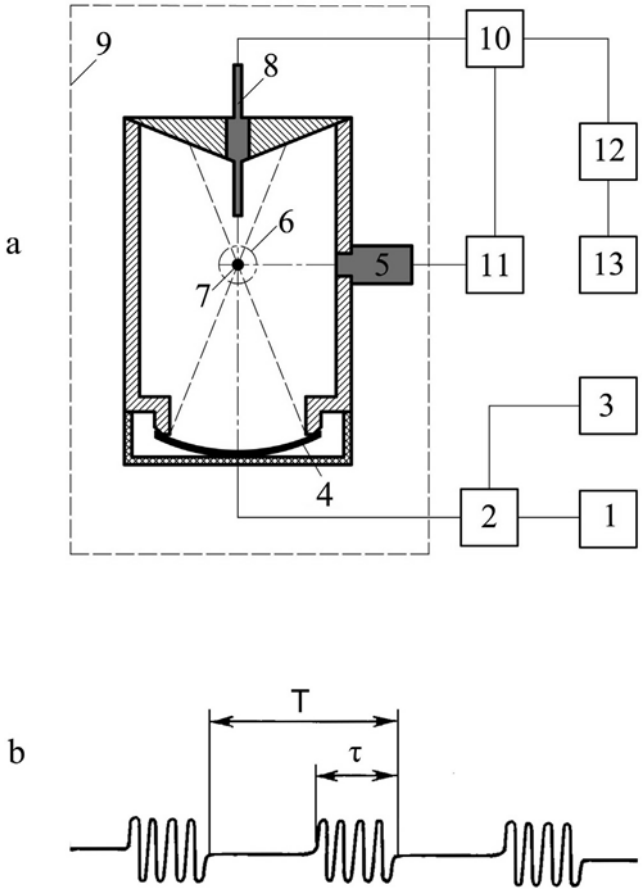


**Fig. 1.** (a) Experimental setup: (1) generator, (2) mixer, (3) pulse generator, (4) transducer, (5) photomultiplier tube, (6) intensive cavitation zone, (7) focal spot of the transducer, (8) hydrophone, (9) light-tight box, (10) preamplifier, (11) oscilloscope, (12) spectrum analyser, (13) PC. (b) Schematic diagram representing the pulse scheme: (T) pulse period of ultrasound pulses, (τ) pulse duration.

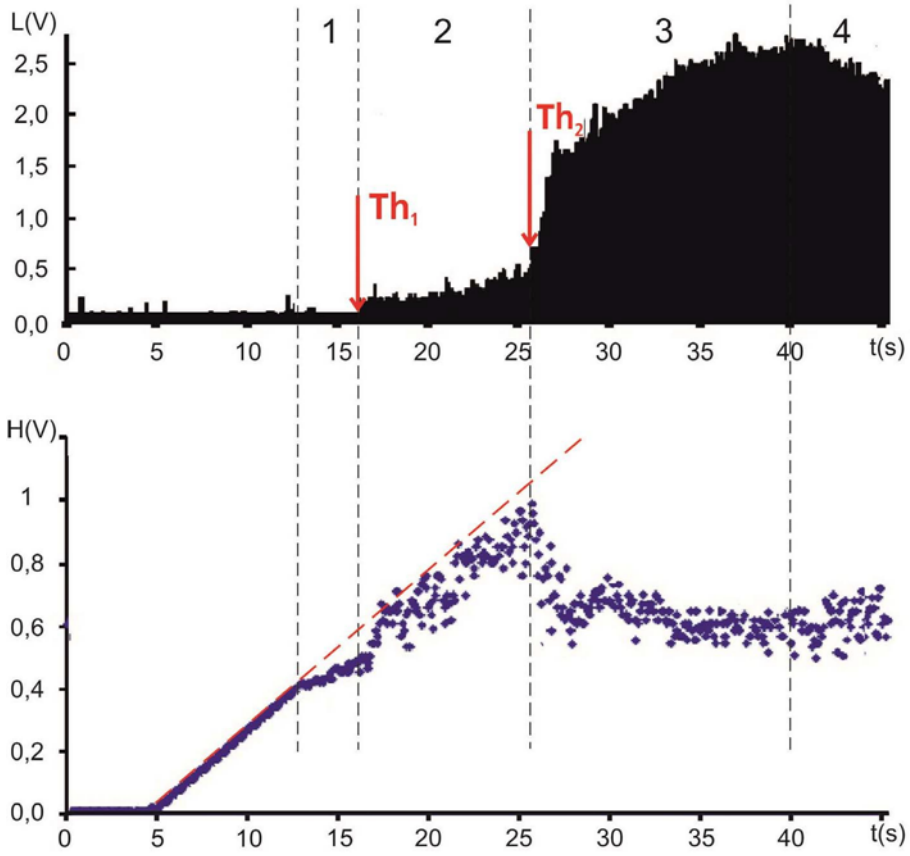


**Fig. 2.** Simultaneous recording of SL intensity L (upper panel), and hydrophone output H (lower panel), T = 30 ms, τ = 3 ms, θ = 23 ± 2 °C. The oscilloscope was operated in peak mode. Cavitation zone stages are separated by dashed vertical lines.

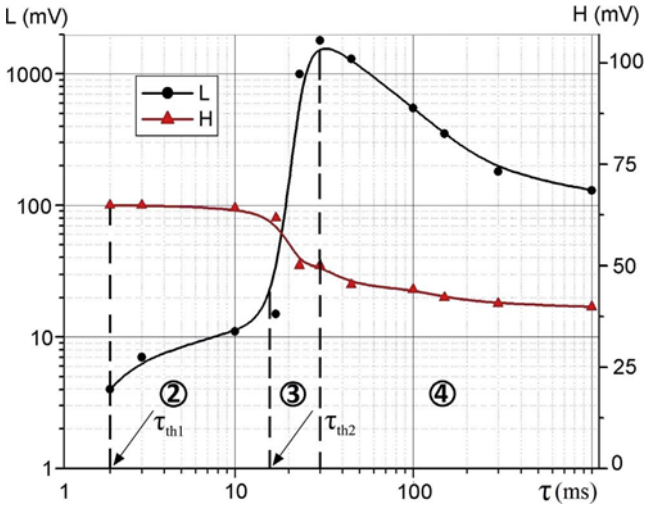


**Fig. 3.** Photomultiplier output, L, and hydrophone output, H, versus ultrasound pulse duration, τ, at ultrasound pulse period T = 100 ms: Up-p = 150 V, θ = 23 ± 1 °C.

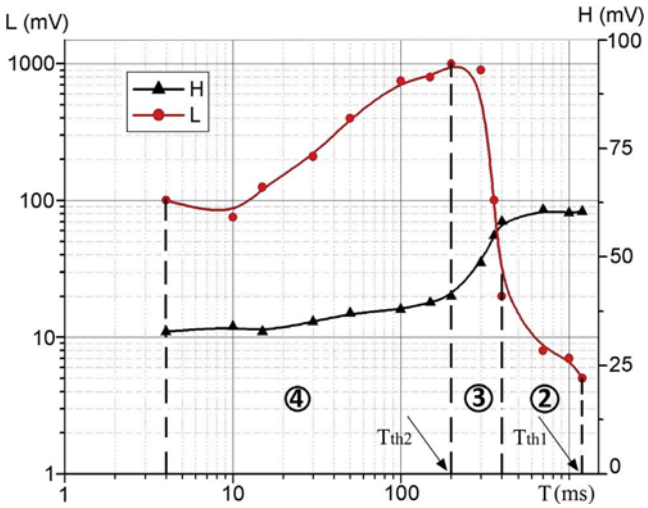


**Fig. 4.** Photomultiplier output, L, and hydrophone output, H, versus ultrasound pulse period T at a pulse duration of $\tau$ = 5 ms: Up-p = 150 V, $\theta$ = 23 ± 1 °C.

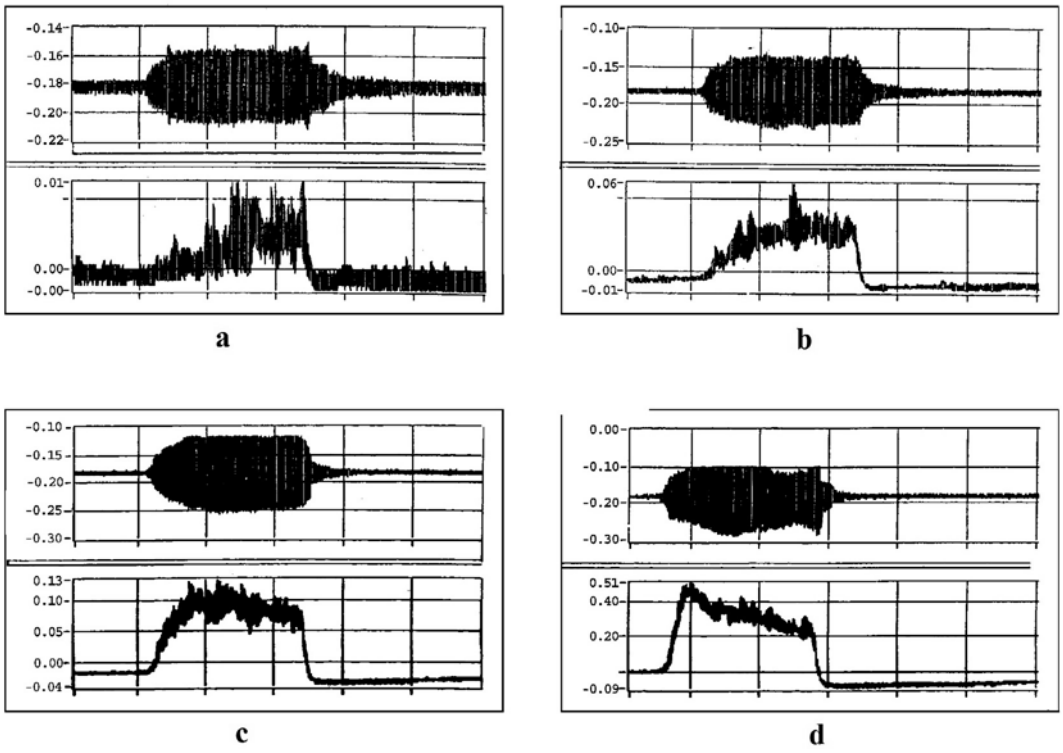


**Fig. 5.** Hydrophone output H (upper diagram in every pair) and photomultiplier output L (lower diagram in every pair) at the different stages of cavitation zone development: (a) the end of stage 1; (b) stage 2; (c) stage 3; (d) stage 4. T = 30 ms, τ = 3 ms, Up-p, V = 105 (a), 175 (b), 210 (c) and 255 (d), θ = 23 ± 1 °C.

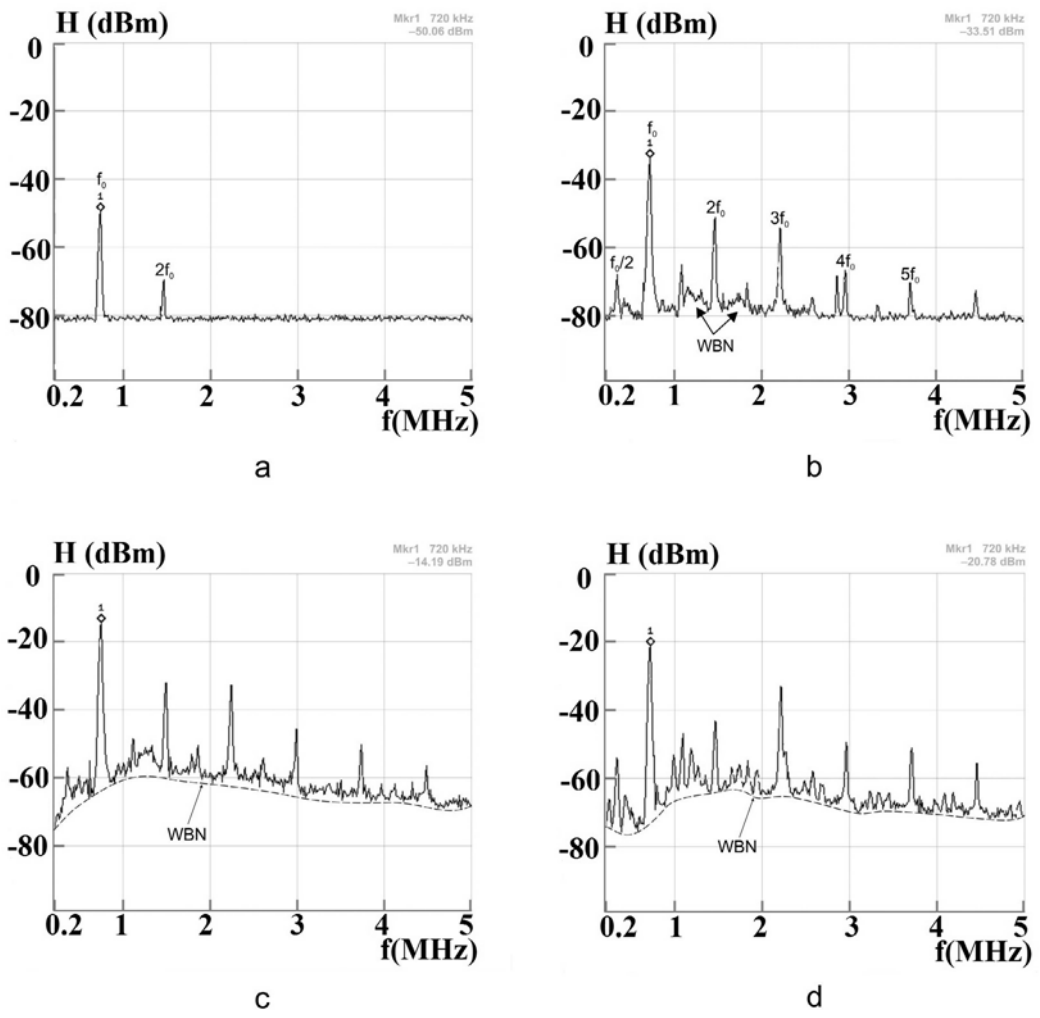


**Fig. 6.** Cavitation noise spectra at different stages of cavitation zone development in the focused ultrasound field: (a) stage one, below SL threshold; (b) stage 2, from SL threshold to a sharp increase in SL intensity; (c) stage 3; (d) stage 4. Pulse period T = 30 ms, pulse duration $\tau$ = 3 ms, $\theta$ = 23 ± 21 °C.